Bioorganic & Medicinal Chemistry Letters 19 (2009) 4555–4559

Contents lists available at ScienceDirect

Bioorganic & Medicinal Chemistry Letters

journal homepage: www.elsevier.com/locate/bmcl

Short-acting 5-(trifluoromethyl)pyrido[4,3-*d*]pyrimidin-4(3*H*)-one derivatives as orally-active calcium-sensing receptor antagonists

Mary T. Didiuk *, David A. Griffith, John W. Benbow, Kevin K. C. Liu, Daniel P. Walker, F. Christopher Bi, Joel Morris, Angel Guzman-Perez, Hua Gao, Bruce M. Bechle, Ryan M. Kelley, Xiaojing Yang, Kenneth Dirico, Syed Ahmed, William Hungerford, Joseph DiBrinno, Michael P. Zawistoski, Scott W. Bagley, Jianke Li, Yuan Zeng, Stephanie Santucci, Robert Oliver, Matthew Corbett, Thanh Olson, Chiliu Chen, Mei Li, Vishwas M. Paralkar, Keith A. Riccardi, David R. Healy, Amit S. Kalgutkar, Tristan S. Maurer, Hang T. Nguyen, Kosea S. Frederick

Pfizer Global Research and Development, 558 Eastern Point Road, Groton, CT 06340, United States

ARTICLE INFO

Article history:
Received 20 March 2009
Revised 25 June 2009
Accepted 2 July 2009
Available online 8 July 2009

Keywords:
Osteoporosis
Human parathyroid hormone
Calcium receptor antagonists
Pharmacokinetics
SAR exploration

ABSTRACT

Synthesis and structure–activity relationship (SAR) studies on 5-trifluoromethylpyrido[4,3-*d*]pyrimidin-4(3*H*)-ones, a novel class of calcium receptor antagonists is described with particular emphasis on optimization of the pharmacokinetic/pharmacodynamic parameters required for a short duration of action compound. Orally-active compounds were identified which displayed the desired animal pharmacology (rapid and transient stimulation of parathyroid hormone) essential for bone anabolic effects.

Osteoporosis is a life-debilitating and prevalent disease associated with significant mortality and morbidity, particularly after hip fracture.[1] In the osteoporotic population, there is an imbalance between bone resorption and bone formation which results in progressive loss of bone mass and structure. Current treatment options involve anti-resorptive agents such as bisphosphonates, estrogen, and selective estrogen receptor modulators, which slow progression of the disease; however, bone which is lost is not restored. In contrast, Teriparatide (Forteo®), a synthetic 1–34 amino acid peptide fragment of human parathyroid hormone (PTH) is the only FDA-approved anabolic agent that, upon daily subcutaneous administration, has been shown to increase bone mineral density and reduce fracture rates in humans.[2–5] As a viable alternative to subcutaneous PTH therapy, one can envision stimulating secretion of endogenous PTH from the parathyroid glands, which is regulated by the calcium receptor (CaR).[6] Proof-of-concept in vivo studies in osteopenic, ovariectomized rats with the aminoalcohol derivative and CaR antagonist NPS 2143 have demonstrated that blockade of CaR results in transient PTH release and stimulation of new bone formation.[7–9]

Key hurdles that preclude clinical studies with NPS 2143 include potent inhibition of human ether-a-go-go (hERG) channel and a long pharmacokinetic half-life ($T_{1/2}$ > 8 h) in animal pharmacology studies that results in significant compound accumulation upon repeated oral dosing. A consequence of the latter is sustained elevation of plasma PTH and a concurrent increase in bone turnover without a net change in bone mineral density.[7,10] This is not unexpected considering that chronically high PTH levels are associated with bone loss (i.e., a catabolic response).[11] While CaR antagonists, structurally diverse from NPS 2143, have been disclosed in the literature, detailed understanding of their in vivo pharmacology in preclinical species, especially in terms of improvement in PTH profile, remains unclear.[10,12] Based upon the studies with NPS 2143, it has been proposed that a rapidly absorbed orally-active agent with a short half-life should evoke the desired transient increase in plasma PTH levels, translating into a bone anabolic response.[10]

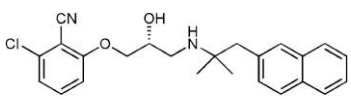

NPS 2143

* Corresponding author. Tel.: +1 860 715 1698.
E-mail address: mary.didiuk@pfizer.com (M.T. Didiuk).

0960-894X/$ - see front matter © 2009 Elsevier Ltd. All rights reserved.
doi:10.1016/j.bmcl.2009.07.004

As a prelude to our discovery efforts, we felt that it was crucial to identify the pharmacokinetic/pharmacodynamic (PK/PD) requirements of a short-acting, orally bioavailable CaR antagonist. Quantitative PK/PD studies were undertaken in rats with a series of literature CaR antagonists (including NPS 2143) to establish a relationship between PTH release and unbound systemic exposures corrected for the corresponding in vitro CaR antagonist potencies (IC_{50}). PTH profiles discerned with small molecule antagonists were then compared with those of Forteo® and Preos® (PTH 1-84, full-length recombinant human PTH) at their respective efficacious doses in the rat, which then allowed an insight into the potency requirements for a small molecule agent.[13,14] Assuming a 1:1 quantitative pharmacology translation between rat and human, simulations were then performed to derive human PK parameters for an orally-active CaR antagonist that would yield PTH profiles similar to the ones discerned with efficacious doses of Forteo and Preos in humans.[15,16] The results of the in-house PK/PD analysis suggested that in order to achieve a Forteo-/Preos-like profile, an orally-active CaR antagonist needs to fulfill the following criteria: (a) in vitro CaR antagonist potency (IC_{50}) $\leqslant$ 50 nM, (b) rapid and complete oral absorption, (c) short half-life ($T_{1/2}$) of $\sim$1 h (ideally achieved via a blood clearance (CL_b) of 10 mL/min/kg and steady state volume (Vd_{ss}) of 1 L/kg).[17,18]

Given the degree of difficulty in achieving the narrow window of human PK properties with any given agent, an overarching goal in this exercise was the identification of multiple candidates with a complementary range of human clearance predictions that would maximize our chances of 'hitting the target' PK range (especially CL and $T_{1/2}$).[19]

For the purposes of pharmacologic and PK optimization, we focused our attention on lead compound **2** (Scheme 1), a pyrido[4,3-*d*]pyrimidin-4(3*H*)-one derivative, related to the previously described 3*H*-quinazolinones class of CaR antagonists.[12a] While potency and predicted human CL for **2** were less than optimal (Table 1), an attractive feature of this compound and chemical series in general was the absence of hERG channel inhibition associated with the amino alcohol series.[10] Herein, we describe our efforts to achieve potency and stringent PK goals for the pyrido[4,3-*d*]pyrimidin-4(3*H*)-ones while seeking to identify multiple compounds suitable for clinical development.

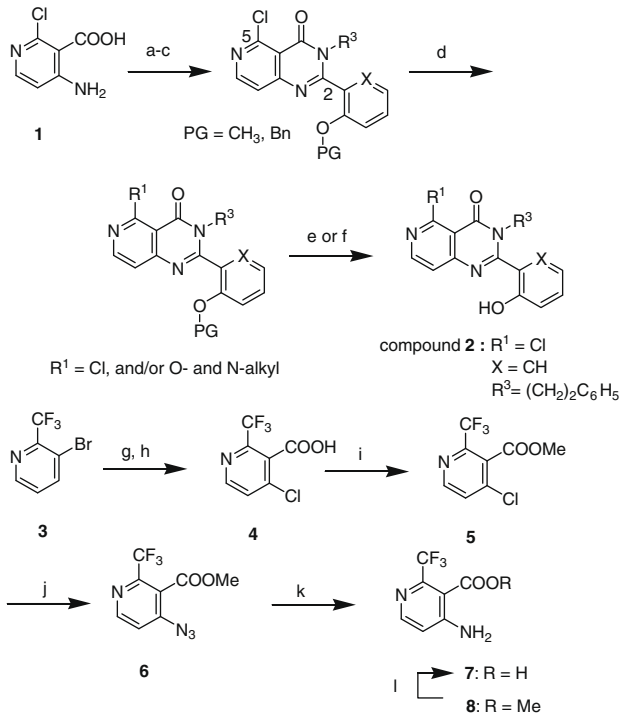

Scheme 1. Reagents and conditions: (a) H_2NR^3, HBTU, Et_3N, CH_2Cl_2/DMF; (b) $CHOArOCH_3$ or CHOArOBn, TsOH, $PhCH_3$, heat; (c) DDQ, CH_2Cl_2 or MnO_2, CH_2Cl_2; (d) *O*-alkyl: ROH, NaH, THF/DMF; *N*-alkyl: R^1NH_2, CH_3OH, 50 °C; (e) BCl_3, CH_2Cl_2; (f) H_2SO_4, AcOH; (g) Mg, THF, reflux, 2 h; CO_2 gas (74%); (h) *n*-BuLi (1.0 equiv), LTMP (3.0 equiv), THF, −78 °C to −50 °C, 1.5 h; C_2Cl_6 (94%); (i) CH_2N_2, EtOAc (99%); (j) NaN_3 (8.0 equiv), DMF, 45–50 °C, 4 h, (98%); (k) HI, 0 °C, 1 h, **7** (48%), **8** (48%); (l) LiOH (1.7 equiv), THF/dioxane/H_2O (3:2:1), 85 °C, 3 h (95%).

Three major areas were examined to improve upon the pharmacology and ADME properties of the pyridopyrimidone series represented by **2**: the C-5 substituent (R_1) with special focus on replacing the potentially electrophilic 2-chloropyridine motif, the C-2 substituent (R_2), and the side chain (R_3). The synthesis of **2** and its analogs is shown in Scheme 1.

The halogen in 2-chloro-4-aminonicotinic acid (**1**) provided a convenient handle for introducing substituents at C-5 and for further SAR exploration. Amidation of **1** with appropriate amines and reaction with either methyl- or benzyl-protected salicylaldehyde analogs afforded 2,3-dihydropyrimidinone derivatives that were oxidized to generate the corresponding pyrido[4,3-*d*]pyrimidin-4(3*H*)-one scaffold. The 5-chloro-analog could be further elaborated with nucleophiles to provide diverse C-5 substituents or O-deprotected to afford **2**. The preparation of 5-trifluoromethyl-pyrido[4,3-*d*]pyrimidin-4(3*H*)-one derivatives was achieved from 2-trifluoromethyl-3-bromopyridine (**3**). Grignard formation from **3** followed by reaction with CO_2 afforded a nicotinic acid derivative, which upon lithiation and treatment with hexachloroethane, afforded **4** in a good yield. Esterification of **4** with diazomethane yielded methyl ester **5**, which was converted to the corresponding azido ester **6** following nucleophilic displacement of the chloride group with sodium azide. Treatment of **6** with concentrated HI afforded a 1:1 mixture of the desired product, 4-amino-2-trifluoromethyl-nicotinic acid (**7**) and its amino ester derivative **8**. The mixture was readily separated via acid–base extraction. Subsequent saponification of **8** with lithium hydroxide provided additional quantities of **7** in 95% yield.

Pyrido[4,3-*d*]pyrimidin-4(3*H*)-ones were evaluated in vitro for human CaR antagonism.[20] Introduction of a range of small alkyl, amino, and ether substituents resulted in compounds with diminished potency when compared with **2** (Table 1). The trifluoromethyl group at C-5 proved ideal, particularly in terms of its

Table 1
SAR on the C-5 substituent in pyrido[4,3-*d*]pyrimidin-4(3*H*)-ones

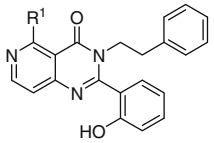

Compound	R^1	CaR IC_{50}[a] (nM)	Log *D*[b]	Predicted human CL_b[c] (mL/min/kg)
2	Cl	106	3.76	4.5
2a		5320	3.77	N.D.
2b		435	4.86	N.D.
2c	$(CH_3)_2CHO$–	224	4.81	5.8
2d	CH_3	2990	3.99	N.D.
2e	CF_3	50	4.89	4.4

[a] Values are means of three experiments.
[b] Values were calculated using ACD/Labs version 9.03.
[c] Human CL_b values were scaled from free CL_{int} data from liver microsomes using the well-stirred model (incorporating unbound fraction in plasma/microsomes) as previously described, Ref. 21.

pharmacology and chemical stability, and was used extensively for further SAR exploration.

The influence of R_2 and R_3 functionalities on potency and microsomal clearance was investigated simultaneously (Table 2). Free intrinsic clearance (CL_{int}) predictions for pyridopyrimidinones and related quinazolinones[12a] obtained from in silico modeling revealed a good correlation (±2-fold error) with experimental values measured in human liver microsomes as shown in Figure 1, a feature which also appeared to be closely governed by Log *D*.[21,22] The

Table 2
SAR on the R_2 and R_3 substituents in pyrido[4,3-*d*]pyrimidin-4(3*H*)-ones

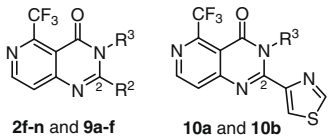

2f-n and **9a-f** **10a** and **10b**

Compound	C-2 (R^2)	R^3	CaR IC_{50}[a] (nM)	Log *D*[b]	Predicted human CL_b[c] (mL/min/kg)
2f	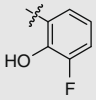	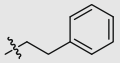	610	4.58	N.D.
2g		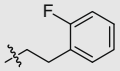	132	4.94	7.3
(*R*)-**2h**		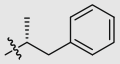	41	5.23	12
(*S*)-**2h**		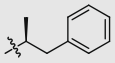	158	5.23	N.D.
2i	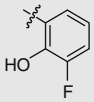	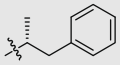	25	4.93	4.0
2j		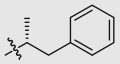	22	3.81	9.0
2k		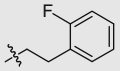	151	3.52	4.0
2l		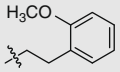	76	3.38	7.5
2m		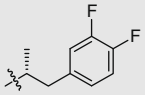	8	3.83	7.4
2n		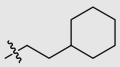	36	4.40	2.0

Table 2 (*continued*)

Compound	C-2 (R^2)	R^3	CaR IC_{50}[a] (nM)	Log *D*[b]	Predicted human CL_b[c] (mL/min/kg)
9a	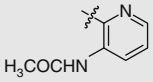	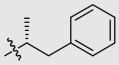	19	5.73	2.0
9b	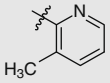	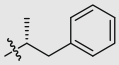	226	4.45	N.D.
9c	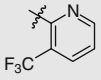	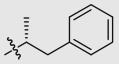	64	5.36	6.0
9d		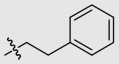	1070	4.80	15
9e		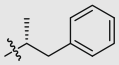	152	5.24	N.D.
9f		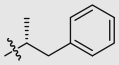	79	4.41	6.7
10a		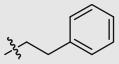	656	3.38	N.D.
10b		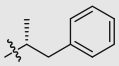	216	4.43	15

N.D. not determined.
[a] Values are means of three experiments.
[b] Values were calculated using ACD/Labs version 9.03.
[c] Protocols for measuring half-lives in human liver microsomes and subsequent scaling of half-life data to intrinsic clearance (CL_{int}) and CL_b have been published, Ref. 21.

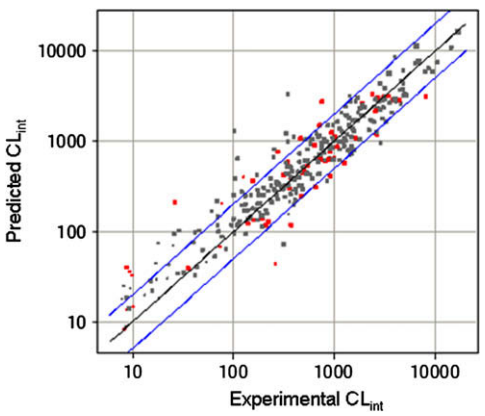

Figure 1. Plot of experimental versus predicted intrinsic liver microsomal clearance (gray dots: training set compounds; red dots: test set compounds).

Table 3
Pharmacokinetic data for selected 5-trifluoropyridopyrimidinones in the rat[a]

Compound	Dose (mg/kg)	Route	RLM CL_p[b]	C_{max} (ng/mL)	T_{max} (h)	CL_p (mL/min/kg)	Vd_{ss} (L/kg)	$T_{1/2}$[c] (h)	AUC (ng h/mL)
(*R*)-**2h**	1	iv	25	125 ± 23	0.5 ± 0.3	32.2 ± 0.92	1.4 ± 0.04	0.6 ± 0.07	518 ± 15
	10	po		350 ± 34					
2i	1	iv	13			31.6	3.60	1.53	528.0
2m	1	iv	28	133 ± 56	0.3 ± 0.1	46.5	8.60[c]	3.90	364.0
	10	po		165 ± 68					
2n	1		33			35.9	3.20	0.62	489.5
9c	1	iv	56	100 ± 50	1.3 ± 0.5	17 ± 4.0	2.9 ± 0.8	0.8 ± 0.06	1200 ± 570
	10	po		450 ± 170					
9f	1	iv	29			21 ± 3.8	6.0 ± 3.8	0.95 ± 0.03	810 ± 160

[a] Pharmacokinetic studies were conducted in male Sprague-Dawley rats (n = 2–5). Compounds were administered in glycerol formal containing 2% DMSO (iv) or as spray dried dispersion (po).
[b] Blood clearance predicted using rat liver microsomes was converted into plasma clearance values by multiplying the blood/plasma partition ratio measured for the individual compounds.
[c] Half-life values represent terminal elimination (β) phase; the effective half-lives (α) were much shorter.

CL_{int} values depicted in Figure 1 are obtained by dividing the apparent liver microsomal CL_{int} values by the unbound fraction of compounds to liver microsomes.[23] The availability of the in silico tool to predict CL of virtual compounds greatly facilitated our efforts toward the design of analogs for SAR purposes.

As indicated in Table 2, subtle changes in the R_2 and R_3 substituents in **2e** affected the balance between potency and CL. For example, incorporation of aromatic fluorine on the phenethyl ring in **2e** generated **2g** with a projected human CL value approaching the target range, albeit with a threefold decrease in CaR potency. Likewise, introduction of a 6′-fluoro group on the phenol substituent in **2e** resulted in **2f** with diminished potency. In the case of **2f**, introduction of a α-methyl group on the 3-phenethyl substituent (compound **2i**) led to a significant boost in potency, wherein the (*R*)-configuration was preferred.

While the introduction of the 6′-fluorine as illustrated in **2f** was detrimental for activity, we were pleased to find that a nitrogen atom at the 3′-position of the C-2 phenol ring was generally well tolerated. When coupled with an appropriate α-methylarylethyl substituent, the change resulted in several compounds with the desired optimal potency and human CL range as highlighted in Table 2. While not extensively investigated in this analysis, the finding that replacement of the pendant arylalkyl group with a cyclohexylethyl moiety (compound **2n**) preserved CaR activity suggests a potential exists for additional SAR work around this region of the molecule. Examination of the influence of Log *D* on potency and clearance predictions on the phenols/3-hydroxypyridine indicated that increased Log *D* values in general correlated with increased potency and higher predicted/measured CL.

The role that the C-2 phenolic hydroxyl group plays in receptor binding remains unclear. Likely hypotheses include hydrogen bonding of the phenol with a complimentary amino acid residue(s) on the receptor in addition to a role in electrostatic interactions with the receptor. The hydrogen bonding contribution was explored by incorporating mildly acidic functionalities (e.g., $NHCOCH_3$) in place of the phenolic OH. Thus, replacement of the OH group in **2j** with the acetamide led to **9a**, which demonstrated comparable CaR potency. The electrostatic component was probed by introducing polarizable functional groups (e.g., Cl or CF_3) in place of the phenolic OH group or by replacing the phenol/3-hydroxypyridine ring system with small heterocycles like thiazole (Table 2).[24,25] In general, replacement of the phenol OH group with small neutral groups/polarizable atoms resulted in compounds with decreased antagonist activity (e.g., **9b** and **9f** vs **2j**). Likewise, replacement of the C-2 phenol/3-hydroxypyridine with the thiazole heterocycle (compound **10a**) also led to a 10-fold loss in potency. A similar finding has been discerned with SAR studies on quinazolinones where the C-2 phenolic compound was far superior to the C-2 furan derivative as a CaR antagonist.[10] As observed earlier, α-methylation of the phenethyl side chain led to a 3–10-fold increase in antagonist activity of the resulting compounds (e.g., **9d**/**9e** and **10a**/**10b**).

Having identified several potent antagonists with a complimentary range of predicted human CL values near the target of 10 mL/min/kg, we examined their in vivo disposition in rats. The purpose of these studies was to establish an in vitro/in vivo correlation for CL to increase confidence in our scaled human CL projections, and to demonstrate PTH release, in vivo. Intravenous (iv) rat PK studies on selected compounds (e.g., (*R*)-**2h**, **2m**, **2n**, **9f**) revealed a good correlation (±2-fold) between observed in vivo CL and the corresponding CL value estimated from rat liver microsomes (Table 3). Pretreatment of rats with the P450 inactivator 1-aminobenzotriazole led to a ~4-fold decrease in clearance of compound (*R*)-**2h** (32.2 → 7.8 mL/min/kg), ~4-fold increase in AUC and a sevenfold increase in half-life, suggesting that oxidative metabolism was the principal elimination pathway in these compounds. Metabolite identification studies on (*R*)-**2h** and **2m** in human and rat liver microsomes and hepatocytes revealed that the rate-limiting step in the metabolism was P450-catalyzed oxidations on the phenol/3-hydroxypyridine motif; glucuronidation of the phenolic OH group in starting material was a very minor component of overall metabolism.[26] Collectively, these observations strengthen the level of confidence level in using human liver microsomes to predict CL of pyridopyrimidinones.

Consistent with previous studies on amino alcohol and quinazolinone-based CaR antagonists,[8,10,12] iv administration of selected compounds (*R*)-**2h** and **2m** at 1 mg/kg (Table 4) to rats resulted in a rapid increase in plasma PTH levels (10–20-fold higher than baseline levels).[27] More importantly, however, were the observations of rapid and transient PTH increases following single po dose

Table 4
PTH stimulation following iv and po administration of 5-trifluoropyridopyrimidinones in the rat[a]

Compound	Dose (mg/kg)	Route	PTH[b,c] (pg/mL)
(*R*)-**2h**	1.0	iv	921
	10	po	620
2m	1.0	iv	1303
	10	po	599

Corresponding levels of the hormone were ~4–6-fold greater than basal levels after po administration.
[a] Studies conducted in male Sprague-Dawley rats (n = 5/6).
[b] PTH levels peaked at ~2 min (earliest sampling point) and at 5 − 15 min in the iv and po studies, respectively.
[c] PTH levels after iv administration were 10–20-fold higher than baseline levels in vehicle treated animals.

administration of (*R*)-**2h** and **2m** at 10 mg/kg. Consistent with the short effective half-lives of the test compounds, PTH elevation was transient and returned to baseline within 60 min following iv or po administration. It is interesting to point out that some compounds (e.g., **2m** and **9f**) exhibited pronounced biphasic kinetics (rapid decline in concentration in the α-phase followed by a prolonged β-phase), leading to higher estimated distribution volumes (>1.0–2.0 L/kg) and longer terminal elimination half-lives. However, this attribute does not result in significant compound accumulation and/or sustained PTH elevation in a sub-chronic setting. For instance, consecutive daily po dosing (10 mg/kg) of (*R*)-**2h** and **2m** in rats for 5 days led to the anticipated transient stimulation of the hormone on days 1 and 5; sustained PTH elevation was not observed on day 5 (comparison with pre-bleed samples with days 1 and 5).

In conclusion, orally-active 5-trifluoromethylpyrido[4,3-*d*]pyrimidin-4(3*H*)-one CaR antagonists with a short duration of action have been identified using a combination of PK/PD and in silico modeling of microsomal stability data, which greatly facilitated design of analogs. Additional safety and ADME profiling is currently underway for analogs (*R*)-**2h** and **2m** in support of potential clinical studies.

References and notes

1. Ray, N. F.; Chan, J. K.; Thamer, M.; Melton, L. J., III *J. Bone Miner. Res.* **1997**, *12*, 24.
2. Nemeth, E. F. *J. Mol. Endocrinol.* **2002**, *29*, 15.
3. Deal, C. *Nat. Clin. Pract. Rheumatol.* **2009**, *5*, 20.
4. Blick, S. K.; Dhillon, S.; Keam, S. J. *Drugs* **2008**, *68*, 2709.
5. Stroup, J.; Kane, M. P.; Abu-Baker, A. M. *Am. J. Health Syst. Pharm.* **2008**, *23*, 1076.
6. (a) Garrett, J. E.; Capuano, I. V.; Hammerland, L. G.; Hung, B. C.; Brown, E. M.; Hebert, S. C.; Nemeth, E. F.; Fuller, F. *J. Biol. Chem.* **1995**, *270*, 12919; (b). *Nat. Rev. Mol. Cell. Biol.* **2003**, *4*, 530.
7. Gowen, M.; Stroup, G. B.; Dodds, R. A.; James, I. E.; Votta, B. J.; Smith, B. R.; Bhatnagar, P. K.; Lago, A. M.; Callahan, J. F.; DelMar, E. G.; Miller, M. A.; Nemeth, E. F.; Fox, J. *J. Clin. Invest.* **2000**, *105*, 1595.
8. Nemeth, E. F.; Delmar, E. G.; Heaton, W. L.; Miller, M. A.; Lambert, L. D.; Conklin, R. L.; Gowen, M.; Gleason, J. G.; Bhatnagar, P. K.; Fox, J. *J. Pharmacol. Exp. Ther.* **2001**, *299*, 323.
9. Arey, B. J.; Seethala, R.; Ma, Z.; Fura, A.; Morin, J.; Swartz, J.; Vyas, V.; Yang, W.; Dickson, J. K., Jr.; Feyen, J. H. M. *Endocrinology* **2002**, *146*, 2015.
10. Yang, W.; Wang, Y.; Roberge, J. Y.; Ma, Z.; Liu, Y.; Lawrence, R. M.; Rotella, D. P.; Seethala, R.; Feyen, J. H. M.; Dickson, J. K., Jr. *Bioorg. Med. Chem. Lett.* **2005**, *15*, 1225.
11. Miller, M. A.; Chin, J.; Miller, S. C.; Fox, J. *Bone* **1998**, *23*, 257.
12. (a) Shcherbakova, I.; Balandrin, M. F.; Fox, J.; Ghatak, A.; Heaton, W. L.; Conklin, R. L. *Bioorg. Med. Chem. Lett.* **2005**, *15*, 1557; (b) Shcherbakova, I.; Huang, G.; Geoffroy, O. J.; Nair, S. K.; Swierczek, K.; Balandrin, M. F.; Fox, J.; Heaton, W. L.; Conklin, R. L. *Bioorg. Med. Chem. Lett.* **2005**, *15*, 2537; (c) Gavai, A. V.; Vaz, R. J.; Mikkilineni, A. B.; Roberge, J. Y.; Liu, Y.; Lawrence, R. M.; Corte, J. M.; Yang, W.; Bednarz, M.; Dickson, J. K., Jr.; Ma, Z.; Seethala, R.; Feyen, J. H. M. *Bioorg. Med. Chem. Lett.* **2005**, *15*, 5478; (d) Yang, W.; Ruan, Z.; Wang, Y.; Van Kirk, K.; Ma, Z.; Arey, B. J.; Cooper, C. B.; Seethala, R.; Feyen, J. H. M.; Dickson, J. K., Jr. *J. Med. Chem.*, **2009**, *52*, 1204.
13. Abraham, A.K.; Mager, D.E.; Gao, X.; Li, M.; Healy, D.R.; Maurer, T.S. *J. Pharmacol. Exp. Ther.* **2009**, *330*, 169.
14. (a) The experimental data was modeled using an indirect response precursor pool PK/PD model, commonly applied to pharmacological mechanisms that result in the stimulation of hormone release into plasma. This modeling effort provided estimates for in vitro potency (IC_{50}) and the maximal fold PTH stimulation above baseline (E_{max}), which would be required for bone anabolism.; (b) Sharma, A.; Jusko, W. J. *Br. J. Clin. Pharmacol.* **1998**, *45*, 229.
15. Schwietert, H. R.; Groen, E. W. J.; Sollie, F. A. E.; Jonkman, J. H. G. *Clin. Pharmacol. Ther.* **1997**, *61*, 360.
16. Hodsman, A. B.; Hanley, D. A.; Ettinger, M. P.; Bolognese, M. A.; Fox, J.; Metcalfe, A. J.; Lindsay, R. *J. Clin. Endocrinol. Metab.* **2003**, *88*, 5212.
17. Half-life ($T_{1/2}$) is calculated as $0.693 \times Vd_{ss}/CL_b$.
18. Assuming complete oral absorption ($F_a = 1$) and insignificant gut metabolism ($F_g = 1$), a theoretical oral bioavailability (F) of 50% is possible with a CL_b of 10 mL/min/kg. Oral F is expressed as a sum of the components: $F_a \times F_g \times F_h$ where F_h is $1 - CL_b/Q$. Q is the human hepatic blood flow at 20 mL/min/kg.
19. Retrospective in-house analysis of success rates for human clearance and half-life predictions using human liver microsomes have revealed ±2-fold error in the predictions.
20. Human embryonic kidney 293 (HEK 293) cells expressing human calcium receptor were used to detect in vitro calcilytic activity using Fluorometric imaging plate reader (FLIPR) methodology. Receptor activation by extracellular Ca^{2+} results in the release of Ca^{2+} from intracellular stores into the cytosol. A fluorescent indicator (Fluo-4) is internalized by the cells from growth media and interacts with Ca^{2+} released into the cytosol to provide means of quantifying intracellular Ca^{2+} levels and receptor agonism/antagonism. Potential antagonists were identified by their ability to decrease this fluorescent response. The IC_{50} values were based on the ability of the cells to inhibit the Ca^{2+} induced increase in intracellular Ca^{2+}. Fluorescence signal was read 42 s after the stimulation of the calcium receptor by the addition of 1.7 mM Ca^{2+} (EC_{95} for calcium).
21. Obach, R. S. *Drug Metab. Dispos.* **1999**, *27*, 1350.
22. In silico model for human microsomal CL was developed based on >500 data points (400 data points for training set and 96 data points for test set). The descriptors used to build the model were: MOE descriptors E-state, lipophilicity and structural fragments coded in MOE. A model describing non-specific microsomal binding using similar descriptors has been published by us. See— Gao, H.; Yao, L.; Mathieu, H. W.; Zhang, Y.; Maurer, T. S.; Troutman, M. D.; Scott, D. O.; Ruggeri, R. B.; Lin, J. *Drug Metab. Dispos.* **2008**, *36*, 2130.
23. Gao, H.; Yao, L.; Mathieu, H. W.; Zhang, Y.; Maurer, T. S.; Troutman, M. D.; Scott, D. O.; Ruggeri, R. B.; Lin, J. *Drug Metab. Dispos.* **2008**, *36*, 2130.
24. Thiazole derivatives **10a** and **10b** were prepared in a similar manner as the corresponding phenolic compounds except thiazole carboxaldehyde was used as a starting material.
25. Title compounds were prepared using the appropriate arylaldehyde derivatives according to the general protocol outlined in Scheme 1.
26. A plausible explanation for lack of significant glucuronidation of the phenolic OH group may be due to the formation of a stable internal H-bond as shown.

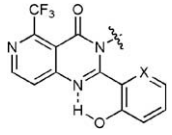

27. Plasma concentrations of PTH 1-84 were measured by using a commercially available PTH ELISA kit, which detects the full length of rat PTH 1-84, specifically.